18èmes Journées Internationales de Thermique (JITH 2017)
Monastir (Tunisie), 25 - 27 Octobre 2017

Analysis and Numerical investigation of the flow characteristics within a solar chimney

Khaled MAHDI, Nadir BELLEL
Laboratoire physique énergétique, université des frères Mentouri, Constantine, Algérie
khaled_mahdi@yahoo.fr, bellelnadir@yahoo.fr

Abstract:

In this present work, the power generation performance in a chimney solar prototype (SCP) was investigated using computational fluid dynamics (CFD). The main objective of this study is to examine the impact of the chimney shape in the power output of a SCP. The CFD analysis is used to determine the location of the turbine using available power. The model is validated by experimental results from the literature review and used as predictive tool. The influence of the absorber temperature, the geometrical shapes of the solar chimney system on the power output of the SCP. These results lead to the better understanding of the impact on these parameters on the thermal updraft wind SCP operating system.

Keywords:

Solar chimney prototype (SCP), CFD, geometrical shapes, updraft wind, Power output.

1. Introduction

In developing the original idea for the purpose of exploiting solar energy, simple techniques in this case, the greenhouse, the chimney and the windmill were combined in an uncomplicated collector and conversion system. Thus the solar chimney was born. The solar chimney power plant concept was originally proposed in 1903 by Isidoro Cabanyes [1]. In 1931, a description of a solar chimney power plant was presented by Günther [2]. The basic study on the solar chimney concept was performed by Schlaich in the 1970s, and in 1981 he began the construction of a 50kW pilot solar chimney power plant in Manzanares, Spain [3,4]. Studying the impact of different components in a solar chimney is a primary task for designing a solar chimney power plant. Haaf et al. [2,3] indicated that the critical roles of chimney height and air temperature in determining the system power output. Pasumarthi et al. [4,6] established a mathematical model for estimating the heat transferring process and the air flow in a SCP. The main controlling parameter investigated was the chimney inclination. The effect of other parameters, curvature effect in the outward (parabolic form) and in the interior (hyperbolic form) on the updraft velocity of the air through a chimney, absorber temperature, has also been investigated. The objective was to use the numerical results to validate the previously proposed correlations and, more importantly, to establish a new empirical correlation that is universally applicable to a wide range of chimney shapes and to increase CSP performance. The analysis described in this communication was originally performed by Motoyama et al. [7,8] and results have been presented in conference papers 4, 5, which have since been cited in new work by other authors.

2. Mathematical and Physical Model

2.1 Experimental model and the configuration

The basic dimension of the SCP was built in Wind Engineering Section at Kyushu University research institute for applied mechanics (RIAM) Japan [7] are as follows:
chimney height for cylindrical and conic shape, 2 m; chimney radius, 0.16 m; collector radius, 1.5 m; height between the inlet of the collector and the center, 0.2 m (as shown in Figure. 1).

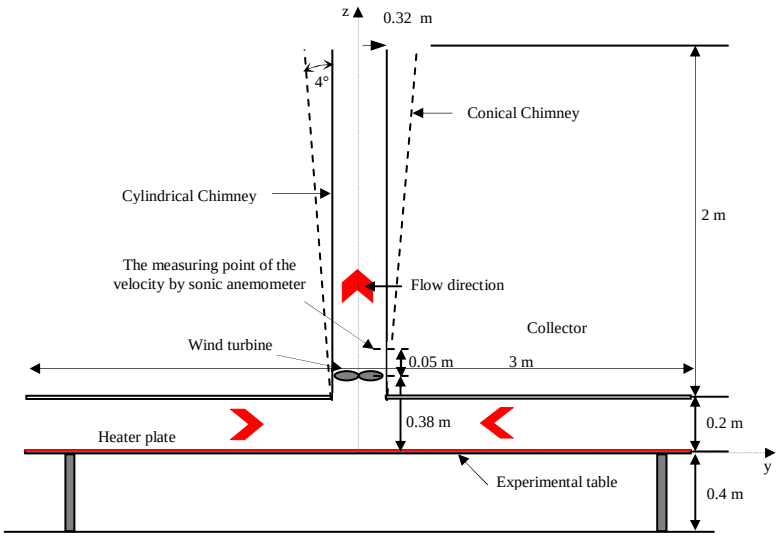

Figure 1: Schematic diagram of a SCP [7]

The collector is made of acrylic and the upper surface is covered with a vinyl sheet from the top so that the ascending wind does not leak out. 8 375 W heater elements are attached to an iron plate of 1.5 m × 1.5 m × 9 mm in thickness using this as a unit panel, 4 panels are combined to form a heater. Based on the results of previous laboratory experiments [3,4], to find an optimal chimney shape, a series of experiments were conducted indoors, as described below. In these experiments, the surface temperature of a heater plate (absorber) at each set point was controlled to maintain constant absorber temperature. Therefore, all the measurements were made under almost steady thermal conditions. The time histories of velocity updraft were recorded for 30 s and its time-mean values were evaluated in the present experiments. An ultrasonic anemometer was installed 50 mm above the wind turbine (see Figure 1).

2.2 Mathematical modelling

In this study the following assumptions are adopted:

- The flow is steady,
- Incompressible fluid. The Boussinesq model is employed and assumes that density can be treated as a constant except in the buoyancy force term ρg,
- The collector surface and chimney surface is assumed under natural convection condition,
- The chimney wall is assumed insulated. The inlet pressure is 101325 pa and the outlet pressure at 2.2 meters chimney height is assumed 101325 pa which is appropriate for such short chimney,
- The gravity in the positive z-direction is – 9.81 m/s^2 while zero on all other direction,
- The temperature of the absorber surface of the collector is assumed to be the same.

Since the purpose of this numerical study is to understand the flow characteristics and the effect of the geometry on the solar chimney performance that was built in RIAM, not the assessment of turbulence models, it is decided that a standard k–ε model would serve the purpose which is also adopted by other study [9,10]. The conservation equations and the standard k–ε turbulent model used in this study is shown below:
Continuity equation:

$$\frac{\partial u_i}{\partial x_i} = 0 \qquad (1)$$

Momentum equation is described by:

$$\rho u_i \frac{\partial u_i}{\partial x_j} = -\frac{\partial p}{\partial x_i} - \rho g_i + \frac{\partial}{\partial x_j}\left[\mu\left(\frac{\partial u_i}{\partial x_j} + \frac{\partial u_j}{\partial x_i}\right)\right] - \rho\overline{u_i' u_j'} \qquad (2)$$

The energy equation in the following form:

$$\rho u_j \frac{\partial T_i}{\partial x_j} = \frac{\partial}{\partial x_j}\left[\frac{\mu}{Pr}\frac{\partial T}{\partial x_j} - \rho\overline{T' u_j'}\right] \qquad (3)$$

Reynolds stresses $\rho\overline{u_i' u_j'}$ in this study are solved using the standard high Reynolds number k–ε model [11] with wall function to resolve the wall bounded effects. The kinetic energy of turbulence,$k = u_i' u_i'/2$, and the rate of dissipation of k, $\varepsilon = (\mu/\rho)\overline{(\partial u_i'/\partial x_j)(\partial u_j'/\partial x_i)}$ are solved using the following transport equations:

$$\rho u_j \frac{\partial k}{\partial x_j} = \frac{\partial}{\partial x_j}\left[\left(\mu + \frac{\mu_t}{\sigma K}\right)\frac{\partial k}{\partial x_j}\right] + P_K - \rho\varepsilon \quad (4)$$

$$\rho u_j \frac{\partial \varepsilon}{\partial x_i} = \frac{\partial}{\partial x_j}\left[\left(\mu + \frac{\mu_t}{\sigma_\varepsilon}\right)\frac{\partial \varepsilon}{\partial x_j}\right] + C_{1S} + C_{1\varepsilon} P_K \frac{\varepsilon}{k} - C_{2\varepsilon}\rho\frac{\varepsilon^2}{k} \quad (5)$$

where, μ_t is the turbulent eddy viscosity, P_K represents the generation of the turbulent kinetic energy and $-\rho\overline{T' u_j'}$ is the turbulent heat flux, which are calculate in equations (7) and (8) respectively.

$$\mu_t = C_\mu \rho \frac{k^2}{\varepsilon} \quad (6)$$

$$P_K = -\rho\overline{u_i' u_j'}\left(\frac{\partial u_j}{\partial x_i}\right) \quad (7)$$

$$-\rho\overline{T' u_j'} = \frac{\mu_t}{\sigma_t}\left(\frac{\partial u_j}{\partial x_i}\right) \quad (8)$$

For the standard k–ε models, the constants have the following values [9]:
$C_{1\varepsilon}$=1.44, $C_{2\varepsilon}$=1.92, C_μ=0.09, σ_k=1.0, σ_ε= 1.3.
Once equations (4) and (5) are solved for k and e, the turbulent Reynolds stress in equation (2) is calculated as follow:

$$-\rho\overline{u_i' u_j'} = \left[\mu_t\left(\frac{\partial u_i}{\partial x_j} + \frac{\partial u_j}{\partial x_i}\right)\right] - \frac{2}{3}\rho k \delta_{ij} \quad (9)$$

The variation of air density due to the heating process was calculated by using the Boussinesq Approximation that only considered the buoyant impact in the body force term in the Navier-Stokes equation [12]:

$$\rho = \rho_0[1 - \beta(T - T_0)] \quad (10)$$

Equation (10) is used to solve for ρ and substituted into the ρg term of Equation (2). The other ρ terms in Equation (2) and (3) are constant equal to ρ_0.
We define power as P_{out} is calculated as follow:

$$P_{out} = \frac{1}{2} C_p \times \rho \times A \times \overline{u}^3 \quad (11)$$

Where, C_p is the power coefficient, A is defined as section of chimney and $\overline{u}$ is represent mean updraft velocity.

2.3 Numerical Procedure

Three chimney shapes different: cylindrical, conic, parabolic and hyperbolic are used for the analysis. Each form is modelled as show in figure 3 using the Gambit tool of Fluent CFD software package [13]. In actual condition of the absorber temperature of the collector, a temperature difference exits between the middle and the edge of the absorber. The air temperature variation exists of the edge at the centre of the absorber caused by the surrounding environment of the experiment. This is because of the natural convection heat loss from the chimney aperture to the ambient. Therefore, in the present numerical analysis a temperature difference (ΔT) of 20, 25, 30, 35 and 40°C has been considered between absorber surface and ambient temperature of the laboratory.
The governing equations are discretized by a second-order upwind numerical scheme, coupled with the SIMPLE algorithm (Semi-Implicit Pressure Linked Equation) and solved using the finite volume method. The pressure-velocity coupling is performed by using the SIMPLE algorithm. Default under-relaxation factors of the solver are employed. The criterion of convergence is that the normalized residuals which are fixed at 1.e–6 for the flow equations. Calculation of the numerical domains has required about 20min of CPU time. The computations were run in Core i5 CPU 2.20 GHz with 8.0 GB of RAM.

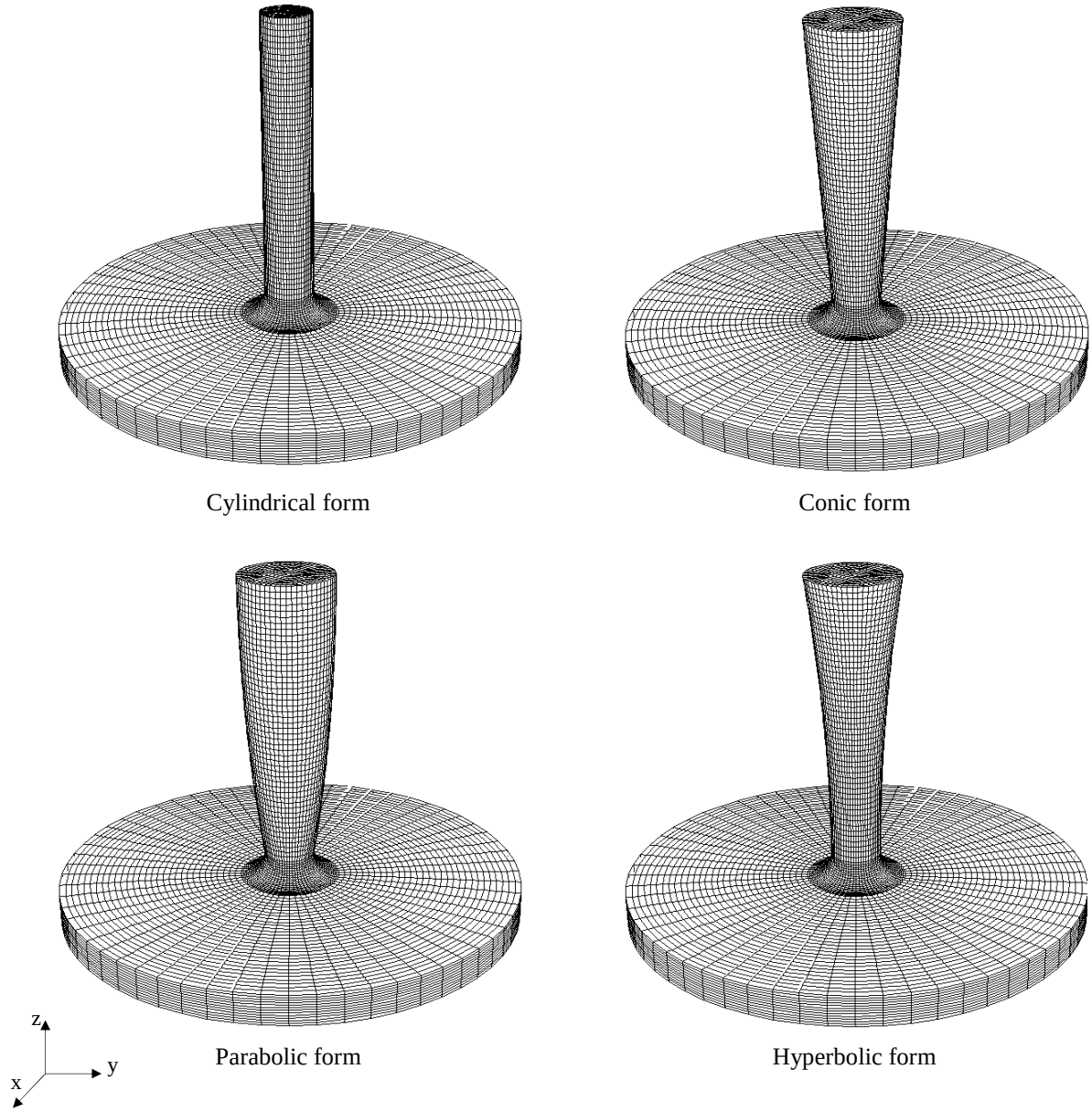

Figure 2: Three-dimensional meshes in four different shapes.

Data for an acrylic sheet and absorber plate in terms of optical factor is illustrated in Table 1.

Table 1: physical properties of walls of the solar chimney prototype

materials	α	ρ	τ	$\rho(kg\times m^{-3})$	$c_p(J\times kg^{-1}\circ\times K^{-1})$	$\lambda(W\times m^{-1}\times K^{-1})$
acrylic sheet	0.06	0.95	0.84	1190	1465	0.19
Absorber plate	0.95	0.95	0	7830	491	70

3. Results and discussion

The numerical simulation was carried out using the FLUENT software which allows simulating a 3D model of a solar chimney prototype. The results were compared with the experimental and numerical data available in the literature to validate the model [7], is shown in figure 3.

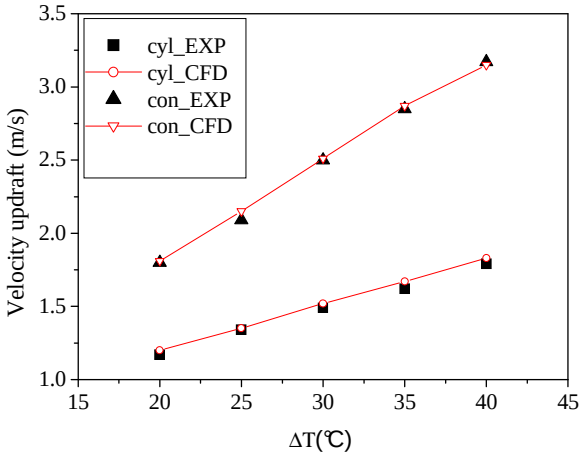

Figure 3: Comparison of velocity between CFD model and sonic anemometer data at point (y = 0, z = 0.42 m)

The velocity of the updraft in the conical chimney exceeded that in the cylindrical chimney. If the rotor of a wind turbine is set at this point, a larger power output is expected. A good agreement between experimental and numerical results was obtained.

Table 2: Curve fitting in the cylindrical and conical chimney and the prediction of optimal geometry

Curve equation	u = A + B×ΔT			
	cyl_EXP	Cyl_CFD	con_EXP	Con_CFD
A	0.570	0.566	0.382	0.458
B	0.030	0.031	0.070	0.068
R^2	0.99905	0.99984	0.99883	0.99915

Figure 4 presents the velocity updraft, static pressure and air temperature through the height of the chimney. We notice that velocities in the three shapes (cylindrical, conic, parabolic and hyperbolic) increase regularly with increasing temperature difference between absorber plate and ambient temperature. In figure 4(a) and 4(b) the maximum of the upward speed can be determined from Table 4 (turbine assembly point). As can be seen in Figure 4(e) and 4(f), temperature is decreased because air flow is rising in the chimney as show in table 3.

The temperature rapidly falls because of the velocity updraft of three forms (conic, parabolic and hyperbolic) compared from cylindrical shape, because as hot air rises with important velocity updraft, air temperature rapidly falls; outer portion of the chimney is insulated from four shapes. Air velocity in collector was slow due to larger height (0.2 m) compared of the chimney radius. And at the point of z = 0.38 m and it rises rapidly at the point z = 0.5 m due to the sudden contraction in chimney sections.

The static pressure parameter can be used as an indicator of the instability zone. As shown in figure 4(c) and 4(d), the minimum negative values of static pressure represent the potentials of the maximum upward velocities in the chimney. This means that the velocities are important in the three forms compared to the cylindrical shape; however, the decrease of the static pressure remains persists in the hyperbolic form and the decrease of the velocity updraft is slow compared to the conic and parabolic forms. Thus, we can say that the hyperbolic form is similar to the cylindrical form (the stable velocity updraft).

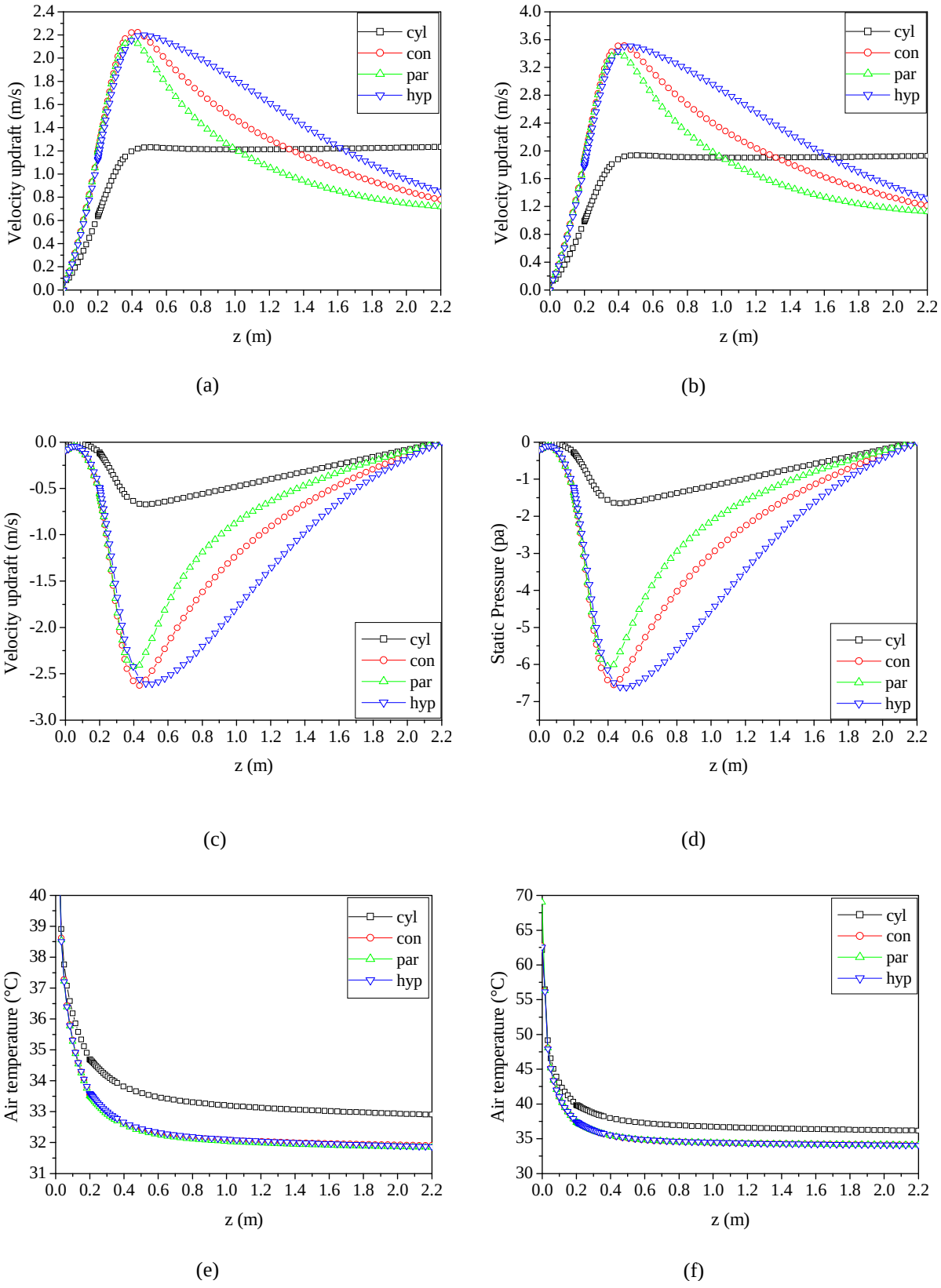

Figure 4: Profiles of air velocity and temperature through the chimney for different shapes of chimney, left: ΔT=20°C, rightΔT=40°C

The power available is expected to increase for the hyperbolic chimney. Figure 5 (b) shows the power available vs. temperature difference. From the results in Figure 11, whereas the ratio of velocity between the hyperbolic shape and cylindrical shape is more 1.8, the power available for the hyperbolic shape turns out to be 5 times greater than for the cylindrical shape. This is because the power output is proportional to the cube of the velocity. In the case of a wind velocity of 2.5 to 3.5 m/s as shown in [8], Cp is the maximum at around a tip speed ratio of. Where Cp = 1.1

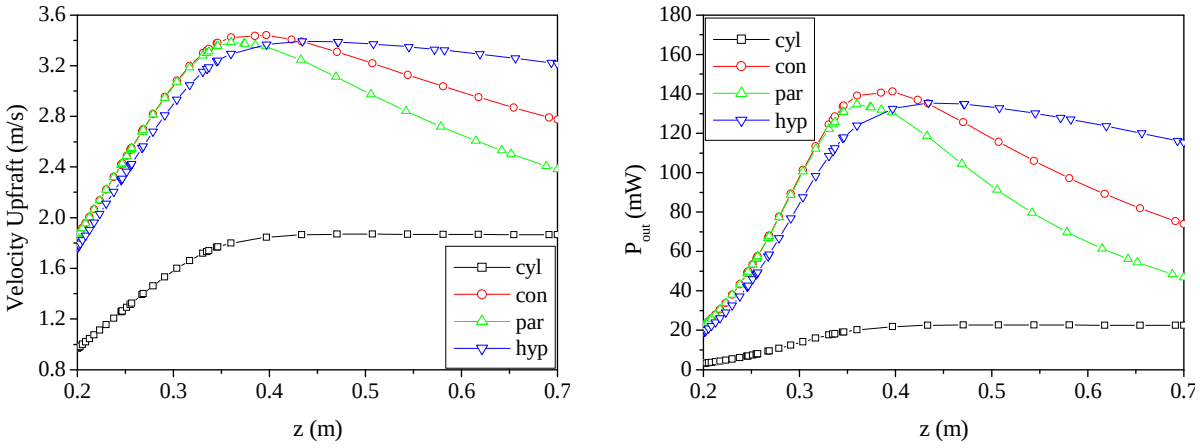

(a) (b)

Figure 5: The effect of chimney shape on the power output

Figure 5 (a) and 5(b) shows the effect of chimney shape and the chimney height on the power available of the system. As analysed above, when the temperature absorber plate is constant, an aperture output of the chimney height causes an increase of the mass flow rate, and the driving force as well. The driving force can be used to drive the axis-based turbine. The increase of driving force will result in the increase of the pressure difference across the turbine. Therefore, the chimney height has a direct effect on the power output of the system. Figure 5 shows distribution of the power available for different chimney shapes and we observed a reasonable agreement with literature

Table 3 shows that the maximum velocity is occurring inside the chimney at different levels, same for Power out and comparative

Table 3: Comparison between the air velocities obtained by CFD simulation

Chimney type	*z(m)*	$u_{max}(m/s)$	$\overline{u}(m/s)$	$P_{max}(mW)$	$\dot{m}$ *(kg/s)*	*ratio*
cyl	0.50	1.87	1.82	22.68	0.1651441	1
con	0.39	3.44	2.43	141.26	0.3182465	4.74
par	0.36	3.38	2.18	134.72	0.3182036	4.12
hyp	0.43	3.39	2.70	135.42	0.3019360	5.63

Conclusion

The investigation of the velocity updraft from solar chimney shapes was undertaken numerically and was validated using the published experimental results for two different chimneys geometries (cylindrical and conical shape). A good agreement between experimental and numerical results was obtained, it is determined that due to the shape of chimney is affected, performance of the system increases positively. In the conclusion one can say that the shape of the conical, parabolic and hyperbolic chimney gives almost the same maximum available power compared with cylindrical shape of the SCP.

We have obtained:

- The available power of the SCP increases with increases of the absorber plate temperature differences.
- The main power available of the SPC hyperbolic is five times greater than the cylindrical SCP.

Nomenclature

Symbol	Nom, *unité*
A	area, m^2
k	kinetic energy of turbulence, m^2/s^2
T	temperature, *K*
u	velocity , *m/s*
$\overline{u}$	mean velocity, *m/s*
P	power, *W*
g	gravity, m/s^2
z	chimney height, *m*
$\dot{m}$	mass rate, *kg/s*
C_p	power coefficient
p	pressure, *pa*
R	correlation coefficient

Greek letters

α	absorptivity
ρ	Reflectivity
τ	transmittivity
ε	rate of dissipation, m^2/s^2
β	thermal expansion coefficient (1/K)
δ_{ij}	kronicer symbol

Exposant, Indices

out	output
max	maximal
m	mean

Acronym

cyl	cylindric
con	conic
par	parbolic
hyp	hyperbolic
EXP	experimental
CFD	computational fluid dynamics
RIAM	research institute for applied mechanics

Références

[1] J. Lorenzo, Las Chimneas solares: de una propuesta espanola en 1903 a de Mansanares, http://www.fotovoltaica.com/chimenea.pdf.

[2] H. Günther, Hundred Years-Future Energy Supply of the World, Franckhsche Verlagshandlung, Stuttgart, Germany, 1931.

[3] W. Haaf, Solar chimneys, part II: preliminary test results from the Manzanares pilot plant, *International Journal of Solar Energy*, volume. 2, Pages 141-161, 1984.

[4] W.Haaf, K. Friedrich, G.Mayr, and J. Schlaich, Solar chimneys, part I: principle and construction of the pilot plant in Manzanares, *International Journal of Solar Energy*, volume 2, Pages 3-20, 1983.

[5] S. W.Yuan, Foundations of Fluid Mechanics, *3rd ed*., *Prentice Hall International*, London, Pages 104-113, 1988.

[6] Fluent 6.2 user guide, Fluent, Inc., Lebanon, NH, 2004.

[7] M. Motoyama, K. Sugitani, Y. Ohya, T. Karasudani, T. Nagai, S. Okada, Improving the power generation performance of a solar tower using thermal updraft wind. *Energy Power Eng*, volume 6, Pages 362-370, 2014.

[8] Motoyama .M, Sugitani K, Ohya Y, Karasudani T, Nagai T And Okada S, *Improvement of power generation on solar tower by thermal updraft wind*, 23rd Conference Wind Engineering , 2014.

[9]R. Sangi, M. Amidpour, B. Hosseinizadeh, Modelling and numerical simulation of solar chimney power plants, *Sol Energy*, Volume85, Pages 829-838, 2011.

[10] T. Ming, W. Liu, G. Xu , Analytical and numerical investigation of the solar chimney power plant systems, *Int. J. Energy Res*, Volume30, Pages 861–873, 2006.

[11] B.E. Launder, D.B. Spalding, The numerical computation of turbulent flows, *Comput Methods Appl. Mech Eng*, Volume 3, Pages 269–289, 1974.

[12] M.O. Hamdan, O. Rabbata, Experimental Solar Chimney Data with Analytical Model Prediction, *in Proceedings of the Solar Conference*, volume 1, Pages 327-332. World Renewable Energy Forum, WREF2012, ISBN:9781622760923, Denver, Colorado, 13–18 May 2012.

[13] Fluent CFD software package, version 6. 3. 26, 2006.